Progress In Electromagnetics Research C, Vol. 115, 245–259, 2021

Novel Sparse Planar Array Synthesis Model for Microwave Power Transmission Systems with High Efficiency and Low Cost

Jianxiong Li[1, 2, *] and Shengjia Chang[1, 2]

Abstract—A novel algorithm is developed to realize the optimal synthesis of a sparse nonuniform-amplitude nonuniform-distribution planar array (SNANDPA) in microwave power transmission (MPT) systems. The dual compression factor particle swarm optimization (DCFPSO) algorithm and the subarray partition technique are adopted to realize the optimal synthesis of SNANDPA. The DCFPSO algorithm first optimizes beam collection efficiency (*BCE*) and side-lobe level outside the receiving region (*CSL*) of SNANDPA which ensure efficient energy transmission of an MPT system and suppress the influence of electromagnetic wave radiated by antenna array on the environment. The subarray partition technique then simplifies the feed network to minimize the system cost. SNANDPA parameters including transmitting aperture, receiving aperture, *BCE*, *CSL*, power pattern, element weight, and element distribution, can be obtained efficiently via the proposed method. Representative numerical cases under the different numbers of subarray and elements conditions are analyzed and compared with those of other two traditional MPT array models. Experimental results show that, when the transmitting aperture is $4.5\lambda \times 4.5\lambda$ and the square receiving region $u_0 = v_0 = 0.2$, *BCE* and *CSL* are 94.96% and -17.09 dB, respectively, and only 64 elements and 8 amplifiers are required. We conclude that the proposed model can be used to create an efficient and low-cost MPT system.

1. INTRODUCTION

Microwave power transmission (MPT) is an innovative technique for long-distance wireless power transfer system. MPT can wirelessly deliver energy from one location to another inaccessible or hazardous location [1–5]. Many scholars have investigated MPT systems [6–10] as per their wide range of potential application scenarios. The transmitting antenna and rectenna are two necessary components for an MPT system; the first concentrates radiated power toward a faraway receiver, while the second collects and converts incoming microwave power [9, 10]. Unlike traditional array systems, MPT systems deal with power transfer rather than information transmission. Efficient energy transmission is vital to an effective MPT system. Although many parameters are related to the total efficiency of MPT system, beam collection efficiency (*BCE*), the ratio of the power obtained by the rectenna to the power radiated by the transmitting antenna, is particularly important.

Strong array performance is necessary to satisfy the demands of MPT system, and system cost should be minimized. Synthesis techniques have been proposed for accomplishing both of these objectives, including transmitting array antenna obtained by stochastic approaches [11–14] and subarray partition technique [15–17]. Besides, the maximum *BCE* for a linear array and planar array can be solved by discrete prolate spheroidal sequences (DPSSs) [18] and generalized eigenvalue problems [19]. Uniform-amplitude nonuniform-distribution planar array (UANDPA) synthesis model in [14] simplifies the array feed network to reduce system cost, but its *BCE* is relatively low at 91.06% which degrades array performance. Nonuniform-amplitude uniform-distribution planar array (NAUDPA) synthesis

Received 24 May 2021, Accepted 13 September 2021, Scheduled 28 September 2021

* Corresponding author: Jianxiong Li (lijianxiong@tiangong.edu.cn).

[1] School of Electrical and Electronics Engineering, Tiangong University, Tianjin, China. [2] Tianjin Key Laboratory of Optoelectronic Detection Technology and Systems, Tianjin, China.

model in [19], for example, achieves *BCE* with 96.45%; however, it needs a large number of array elements and has a "quasi-Gaussian" excitation distribution which raises system cost.

Sparse array, which has larger element distance and fewer elements than fully populated array, is of considerable interest in a large number of applications, such as radar and MPT. It can effectively reduce the cost of the array while ensuring the performance of the array. Previous works have been done to realize the sparse optimization through Compress Sensing (CS) technique [23], convex optimization [24], and stochastic optimization [25–27]. Though it can be used to effectively realize the sparse distribution of array elements, CS technique is applied to small or medium-sized arrays [23]. Convex optimization technology solves the problems existing in CS technique to a certain extent, but there are still defects in *BCE* [24]. Due to these facts, many researchers focus on stochastic optimization [25–27].

Previous studies on this subject have tended to center on simply optimizing array performance or system cost individually. Thus, previously presented methods tend to have performance defects or cost defects. In this paper, a sparse array synthesis method considering both array performance and system cost is proposed. The proposed method first applies the dual compression factor particle swarm optimization (DCFPSO) [20, 21] to improve sparse array performance by optimizing *BCE*, and then simplifies the feed network with a subarray partition technique. In consequence, the optimized synthesis model of sparse nonuniform-amplitude nonuniform-distribution planar array (SNANDPA) is obtained.

2. MATHEMATICAL DERIVATION OF THE MAXIMUM BCE

The physical model of MPT system is shown in Fig. 1. The mathematical derivation of the maximum *BCE* is presented in this section.

Assume that an MPT system has $N = N_x \times N_y$ radiating elements separately distributed on the coordinates (x_n, y_n), $n = 1, 2, ..., N$, where the radiating elements are distributed on the antenna surface with the aperture of $L_x \times L_y$ on the XOY plane. The rectenna is located in far-field zone. The array

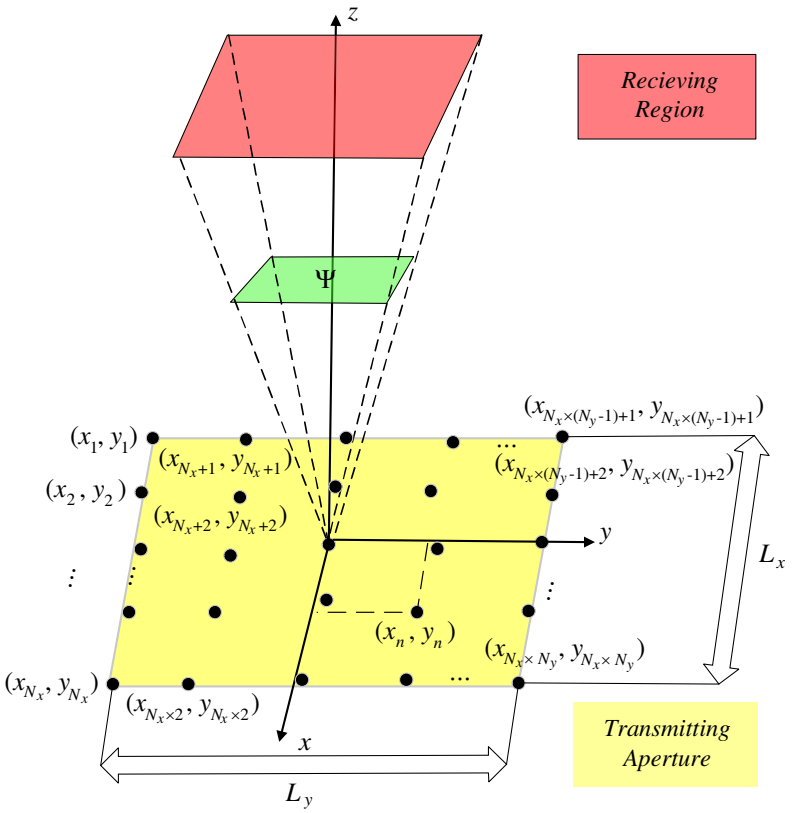

Figure 1. Physical model of MPT system.

factor can be defined as:

$$F(u,v) = \sum_{n=1}^{N} w_n e^{ik(ux_n+vy_n)} \tag{1}$$

where $u = \sin\theta\cos\varphi$ and $v = \sin\theta\sin\varphi$ are direction parameters; w_n represents element weight; $k = (2\pi/\lambda)$ is the wave number; and λ is the wavelength. $e^{ik(ux_n+vy_n)}$ can be defined as $v_n(u,v)$ so that the array factor can be rewritten as

$$F(u,v) = \sum_{n=1}^{N} w_n v_n(u,v) \tag{2}$$

As a matter of convenience, we can rewrite Eq. (2) in matrix form as

$$F(u,v) \triangleq \mathbf{w}^H \mathbf{v}(u,v) \tag{3}$$

where $\mathbf{w} \triangleq [w_1, w_2, ..., w_N]^H$ and $\mathbf{v}(u,v) = [e^{-ik(ux_1+vy_1)}, e^{-ik(ux_2+vy_2)}, ..., e^{-ik(ux_N+vy_N)}]^H$ are weight vector and steering vector, respectively. The superscript "H" indicates complex-conjugate transpose. *BCE* is expressed as:

$$BCE \triangleq \frac{P_\Psi}{P_\Omega} = \frac{\displaystyle\int_\Psi |F(u,v)|^2 dudv}{\displaystyle\int_\Omega |F(u,v)|^2 dudv} \tag{4}$$

where $P_S = \int_S |F(u,v)|^2 dudv$ denotes the power flowing through the angular region $S = \{\Psi, \Omega\}$ where Ψ and $\Omega \triangleq \{(u,v) : u^2 + v^2 \le 1\}$ are the $(u,\ v)$ — angular region identifying the radiated area and the whole visible range, respectively. Eq. (5) is obtained by substituting Eq. (3) into Eq. (4):

$$BCE = \frac{\displaystyle\int_\Psi \mathbf{w}^H \mathbf{v}(u,v)\mathbf{v}^H(u,v)\mathbf{w} dudv}{\displaystyle\int_\Omega \mathbf{w}^H \mathbf{v}(u,v)\mathbf{v}^H(u,v)\mathbf{w} dudv} = \frac{\mathbf{w}^H \mathbf{A} \mathbf{w}}{\mathbf{w}^H \mathbf{B} \mathbf{w}} \tag{5}$$

where $\mathbf{A} \triangleq [\int_\Psi \mathbf{v}(u,v)\mathbf{v}^H(u,v) dudv]$ is the receiving matrix of the system, and $\mathbf{B} \triangleq [\int_\Omega \mathbf{v}(u,v)\mathbf{v}^H(u,v) dudv]$ is the transmitting matrix of the system.

Based on Eq. (5), the optimal weight vector of the elements, $\mathbf{w}^{\text{opt}}$, is determined as

$$\mathbf{w}^{\text{opt}} = \arg\left[\max_{\mathbf{w}} \left(\frac{\mathbf{w}^H \mathbf{A} \mathbf{w}}{\mathbf{w}^H \mathbf{B} \mathbf{w}}\right)\right] \tag{6}$$

According to the optimal theoretical synthesis in [19], the maximum *BCE* and its corresponding weight can be obtained by calculating the generalized eigenvalues and corresponding generalized eigenvectors of the matrix equation. The matrix equation is:

$$\mathbf{A}\mathbf{w}^{\text{opt}} = BCE_{\max} \mathbf{B} \mathbf{w}^{\text{opt}} \tag{7}$$

where $BCE_{\max}$ (maximum *BCE*) is the maximum generalized eigenvalue of Eq. (7) and $\mathbf{w}^{\text{opt}}$ the corresponding eigenvector. The closed-form solution of receiving matrix $\mathbf{A}$ and transmitting matrix $\mathbf{B}$ can be seen in the Appendix.

3. OPTIMAL SYNTHESIS OF SNANDPA WITH HIGH *BCE* AND LOW COST

3.1. SNANDPA Synthesis of Transmitting Array

Section 2 introduces the optimal theoretical synthesis of planar array [19], which can solve the maximum *BCE* and optimal element weight of array. Reference [19] only discussed the fully populated uniform distribution condition, but the optimization of the array element position was not considered. In this

study, we develop an optimal SNANDPA synthesis method which optimizes the distribution and the weight of elements simultaneously.

The stochastic algorithm can be used to solve the planar array synthesis problem to obtain an optimal SNANDPA model. Eq. (7) indicates that every array distribution has a corresponding optimal weight. The array excitation can thus be optimized via the optimization of the array distribution. The correlation between the distribution and the weight of array elements in Eq. (7) can be helpful for simultaneously optimizing both the array distribution and the array weight, which give the optimized model strong array performance. Therefore, the optimal generalized eigenvalue in Eq. (7) is used here as the fitness function of a stochastic algorithm. The optimization model can be expressed as:

$$\begin{cases} \text{find} & \mathbf{X} = [x_1, x_2, ..., x_n, ..., x_N, y_1, y_2, ..., y_n, ..., y_N] \\ \text{maximize} & f(\mathbf{X}) = BCE_{\max}(\mathbf{X}) \\ \text{subject to} & (a)\ \sqrt{(x_n - x_m)^2 + (y_n - y_m)^2} \geq d_{\min} \\ & \quad m \neq n,\ and\ m, n \in \{1, 2, ..., N\} \\ & (b)\ -L_x/2 \leq x_n \leq L_x/2,\ n = \{1, 2, ..., N\} \\ & \quad -L_y/2 \leq y_n \leq L_y/2,\ n = \{1, 2, ..., N\} \end{cases} \tag{8}$$

We use the DCFPSO algorithm [20, 21] to find the optimal element distribution, $\mathbf{X}$, and the corresponding optimal element weight, $\mathbf{w}^{\text{opt}} \triangleq [w_1^{\text{opt}}, w_2^{\text{opt}}, ..., w_n^{\text{opt}}, ..., w_N^{\text{opt}}]^H$. In the process of optimization, the optimal element distribution is constrained by the minimum element distance, $d_{\min}$, and array apertures, $L_x \times L_y$. This model realizes an optimal synthesis of transmitting array, but due to the inadequate consideration of the relationship between the array apertures constrain and minimum element distance constrain, the search for the optimal element distribution is still difficult. To remedy this, we rewrite the decision variables, $\mathbf{X}$, with two matrixes

$$\begin{aligned} \mathbf{X} \triangleq & \begin{bmatrix} x_1 & x_{N_x+1} & \cdots & x_{N_x\times(N_y-1)+1} \\ x_2 & x_{N_x+2} & \cdots & x_{N_x\times(N_y-1)+2} \\ \vdots & \vdots & & \vdots \\ x_{N_x} & x_{N_x\times 2} & \cdots & x_{N_x\times N_y} \\ y_1 & y_{N_x+1} & \cdots & y_{N_x\times(N_y-1)+1} \\ y_2 & y_{N_x+2} & \cdots & y_{N_x\times(N_y-1)+2} \\ \vdots & \vdots & & \vdots \\ y_{N_x} & y_{N_x\times 2} & \cdots & y_{N_x\times N_y} \end{bmatrix} \\ = & \begin{bmatrix} d_{x_1} & d_{x_{N_x+1}} & \cdots & d_{x_{N_x\times(N_y-1)+1}} \\ d_{x_2} & d_{x_{N_x+2}} & \cdots & d_{x_{N_x\times(N_y-1)+2}} \\ \vdots & \vdots & & \vdots \\ d_{x_{N_x}} & d_{x_{N_x\times 2}} & \cdots & d_{x_{N_x\times N_y}} \\ d_{y_1} & d_{y_{N_x+1}} & \cdots & d_{y_{N_x\times(N_y-1)+1}} \\ d_{y_2} & d_{y_{N_x+2}} & \cdots & d_{y_{N_x\times(N_y-1)+2}} \\ \vdots & \vdots & & \vdots \\ d_{y_{N_x}} & d_{y_{N_x\times 2}} & \cdots & d_{y_{N_x\times N_y}} \end{bmatrix} + \begin{bmatrix} 0 & 0 & \cdots & 0 \\ d_{\min} & d_{\min} & \cdots & d_{\min} \\ \vdots & \vdots & & \vdots \\ (N_x-1)\times d_{\min} & (N_x-1)d_{\min} & \cdots & (N_x-1)\times d_{\min} \\ 0 & d_{\min} & \cdots & (N_y-1)\times d_{\min} \\ 0 & d_{\min} & \cdots & (N_y-1)\times d_{\min} \\ \vdots & \vdots & & \vdots \\ 0 & d_{\min} & \cdots & (N_y-1)\times d_{\min} \end{bmatrix} \\ = & \begin{bmatrix} (\mathbf{D_x})_{N_x\times N_y} \\ (\mathbf{D_y})_{N_x\times N_y} \end{bmatrix} + \begin{bmatrix} (\mathbf{D_{min\_x}})_{N_x\times N_y} \\ (\mathbf{D_{min\_y}})_{N_x\times N_y} \end{bmatrix} \end{aligned} \tag{9}$$

where X decision matrix, $\mathbf{D_x}$, represents x-direction decision variables of the array; Y decision matrix, $\mathbf{D_y}$, is the y-direction decision variables of the array; $\mathbf{D_{min\_x}}$ is the minimum element spacing matrix in x-direction and $\mathbf{D_{min\_y}}$ minimum element spacing matrix in the y-direction. Through Eq. (9), we

can obtain the following model:

$$\begin{cases} \text{find} & \mathbf{D} = \begin{bmatrix} \mathbf{D_x} \\ \mathbf{D_y} \end{bmatrix} \\ \text{maximize} & f(\mathbf{D}) = BCE_{\max}(\mathbf{D}) \\ \text{subject to} & (a)\, -L_x/2 \le d_{x_{N_x\times i+1}} < d_{x_{N_x\times i+2}} < ... < d_{x_{N_x\times i+N_x}} \le L_x/2 - (N_x-1)d_{\min} \\ & \quad (i = 0, 1...N_y - 1) \\ & (b)\, -L_y/2 \le d_{y_{1+i}} < d_{y_{N_x+1+i}} < ... < d_{y_{N_x\times(N_y-1)+1+i}} \le L_y/2 - (N_y-1)d_{\min} \\ & \quad (i = 0, 1...N_x - 1) \\ & (c)\, d_{x_1} = d_{x_{N_x\times(N_y-1)+1}} = -L_x/2, d_{y_1} = d_{y_{N_x}} = -L_y/2 \\ & (d)\, d_{x_{N_x}} = d_{x_{N_x\times N_y}} = L_x/2 - (N_x-1)d_{\min} \\ & \quad d_{y_{N_x\times(N_y-1)+1}} = d_{y_{N_x\times N_y}} = L_y/2 - (N_y-1)d_{\min} \end{cases} \tag{10}$$

As a result, the decision variables change from $\mathbf{X}$ to $\mathbf{D}$. Through this way, the unconstrainted particle distribution, (x_n, y_n), can be indirectly transformed into constrained particle distribution, (d_{x_n}, d_{y_n}), and the search space can be reduced from $\{[-L_x/2, L_x/2], [-L_y/2, L_y/2]\}$ to $\{[-L_x/2, L_x/2 - (N_x - 1)d_{\min}], [-L_y/2, L_y/2 - (N_y - 1)d_{\min}]\}$. Finally, the difficulty of searching the optimal decision variable is overcome, and the synthesis problem can be solved more efficiently.

In this subsection, we use the optimal generalized eigenvalue (Section 2) as the fitness value of the stochastic algorithm, then convert the array synthesis problem into an optimization problem formulated in Eq. (7) which allowed us to obtain the optimal distribution of the array, $\mathbf{X}$, and optimal elements weight, $\mathbf{w}^{\text{opt}}$, of SNANDPA simultaneously. After the problem formulation, we adopt a decision variables conversion strategy and convert the decision variables from $\mathbf{X}$ to $\mathbf{D}$. Finally, the array performance of MPT system can be markedly improved by this approach.

3.2. Subarray Partition Technique for Transmitting Array

The optimization of radiating elements can be realized by a stochastic algorithm as discussed in Subsection 3.1. However, the resultant "quasi-Gaussian" excitation distribution increases the cost of the array antenna, which limits the application of the algorithm in actual engineering scenarios. We next attempt to optimize both the array performance and the system cost of the planar array simultaneously by using a subarray partition technique. Through this technique, we can solve "quasi-Gaussian" excitation distribution problem while maintaining relatively strong array performance.

The proposed subarray partition technique works by dividing N elements into M subarray according to the optimal element weight $\mathbf{w}^{\text{opt}}$. According to this idea, we first obtain an $N \times M$ matrix, $\mathbf{R}$, which is given by

$$\mathbf{R} = \begin{bmatrix} R_{11} & R_{12} & \cdots & R_{1M} \\ R_{21} & R_{22} & \cdots & R_{2M} \\ \vdots & \vdots & \ddots & \vdots \\ R_{N1} & R_{N2} & \cdots & R_{NM} \end{bmatrix} \tag{11}$$

Then we initialize the weight range, $\mathbf{w}^{\text{range}} \triangleq [w_0^{\text{range}}, w_1^{\text{range}}, ..., w_M^{\text{range}}]^H$, which can be calculated by

$$w_m^{\text{range}} = w_{\min}^{\text{opt}} + \frac{w_{\max}^{\text{opt}} - w_{\min}^{\text{opt}}}{M} \times m, \quad (m = 0, 1, ..., M) \tag{12}$$

where $w_{\max}^{\text{opt}}$ and $w_{\min}^{\text{opt}}$ are the maximum value and minimum value of $\mathbf{w}^{\text{opt}}$, respectively. In order to define the matrix, $\mathbf{R}$, we set the values of the elements in $\mathbf{R}$ by the following rule

$$\begin{cases} \text{if} \quad w_{m-1}^{\text{range}} \le w_n^{\text{opt}} \le w_m^{\text{range}}, & R_{nm} = 1 \\ \text{else}, & R_{nm} = 0 \end{cases} \tag{13}$$

Through this way, we can realize the initialization of the matrix $\mathbf{R}$. With the help of this matrix, we can concisely describe the results of the subarray partition. Then we initialize the value of the subarray

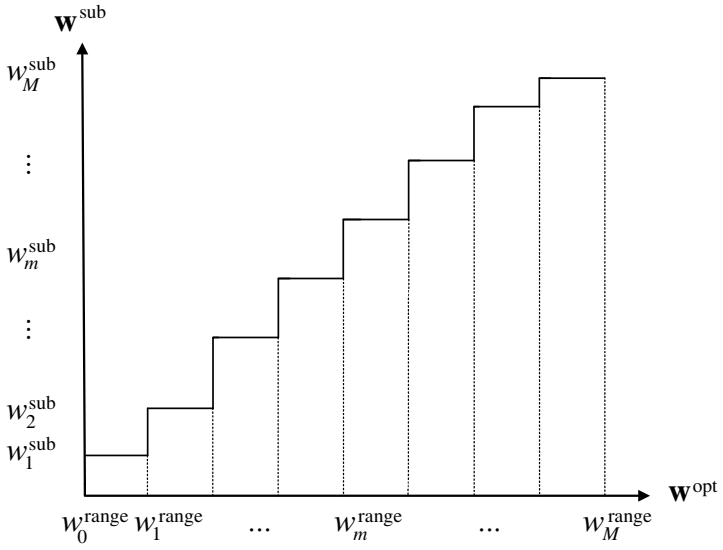

Figure 2. Schematic of SAD.

weight $\mathbf{w}^{\text{sub}} \triangleq [w_1^{\text{sub}}, w_2^{\text{sub}}, ..., w_M^{\text{sub}}]^H$ by solving the following formulation:

$$w_m^{\text{sub}} = \frac{\sum_{n=1}^{N} R_{nm} \cdot w_n^{\text{opt}}}{\sum_{n=1}^{N} R_{nm}}, \quad (m = 1, 2, ..., M) \tag{14}$$

The optimal solution of SNANDPA obtained by this initialization is more stable than that obtained by random initialization. And the resultant stepped amplitude distribution (SAD) schematic is shown in Fig. 2. After that, we can obtain the optimal subarray weight $\mathbf{w}^{\text{sub}}$ through a modified tabu search (MTS) algorithm [22]. And the optimization model can be expressed as:

$$\begin{cases} \text{find} & \mathbf{w}^{\text{sub}} = [w_1^{\text{sub}}, w_2^{\text{sub}}, ..., w_m^{\text{sub}}, ..., w_M^{\text{sub}}]^H \\ \text{maxmize} & f(\mathbf{w}^{\text{sub}}) = BCE_{\max}(\mathbf{w}^{\text{sub}}) \\ \text{subject to} & (a)\, w_{\min}^{\text{opt}} \le w_1^{\text{sub}}, w_M^{\text{sub}} \le w_{\max}^{\text{opt}},\ m = 1, ..., M \\ & (b)\, w_1^{\text{sub}} < w_2^{\text{sub}} < ... < w_m^{\text{sub}} < ... < w_M^{\text{sub}},\ m = 1, ..., M \end{cases} \tag{15}$$

In this model, the optimal subarray weight, $\mathbf{w}^{\text{sub}}$, of the SNANDPA model is determined by the MTS algorithm. In the process of optimization, the optimal subarray weight is constrained by the previous optimal element weight $\mathbf{w}^{\text{opt}}$ and the inner relation of its element. Finally, we can obtain the optimal element weight after subarray partition,$\mathbf{w}^{\text{final}}$, which can be expressed as follows

$$\mathbf{w}^{\text{final}} = \mathbf{R} \cdot \mathbf{w}^{\text{sub}} \tag{16}$$

In this subsection, we use the MTS algorithm to realize the conversion of excitation distribution from "quasi-Gaussian" to SAD and find the optimal element weight after subarray partition $\mathbf{w}^{\text{final}}$. This process makes the SNANDPA model simplify the feed network, reduce the system cost, and maintain good array performance.

4. SIMULATIONS AND NUMERICAL RESULTS

We conduct a series of simulations to examine the feasibility and effectiveness of the proposed model. First, we use the proposed method to synthesize SNANDPAs with different sparsity parameters. Second,

to validate the SNANDPA model, we compare the numerical results of the proposed model with those of other two models under the same parameters: UANDPA [14] and NAUDPA [19]. Third, we compare the DCFPSO algorithm and other PSO algorithms in terms of the performance. The PC used for all simulations has an Intel Core i7-4510U CPU with 2.0 GHz and 8 GB Ram. We use MATLAB R2019b software for all simulations.

We use two evaluation indicators to intuitively compare the results. One is *BCE*, and the other is *CSL* defined as:

$$CSL\,(\mathrm{dB}) = 10\lg\frac{\max_{u,v\notin\Psi}|F(u,v)|^2}{\max_{u,v\in\Omega}|F(u,v)|^2} \tag{17}$$

Assume that the receiving region is a rectangular area facing the transmitting array:

$$\Psi \triangleq \{(u,v) : -u_0 \le u \le u_0, -v_0 \le v \le v_0\} \tag{18}$$

And the visible range of the transmitting array is the hemisphere facing the receiving region:

$$\Omega \triangleq \left\{[u(\theta,\varphi), v(\theta,\varphi)] : \theta \in [0,\frac{\pi}{2}], \varphi \in [0,2\pi]\right\} \tag{19}$$

We also define two sparsity parameters. One is the ratio of amplifier sparsity γ_a, i.e., the ratio of the amplifier number of the array to the element number of the array. The other is the ratio of element sparsity γ_e, i.e., the ratio of the element number of the sparse array to that of the fully populated array.

4.1. Effects of Different Sparsity Parameters on Synthesized Results

As mentioned in Section 1, the transmitting antenna and receiving antenna are two key components of the SNANDPA model. This paper focuses on the effect of γ_a and γ_e in the SNANDPA model, so we set transmitting aperture as $L_x = L_y = 4.5\lambda$ and receiving region as $u_0 = v_0 = 0.2$. This allows us to focus on the optimization of the sparsity parameters γ_a and γ_e.

The value of subarray M determines the ratio of amplifier sparsity γ_a of SNANDPA. To find an optimal subarray value M_{opt} of the SNANDPA model, we investigate the influence of M on synthesized results of the SNANDPA model. We select an array with $N = 8\times 8$ and set the value of minimum element distance $d_{\min}$ as the half wavelength $\lambda/2$. We find that the performance of the array becomes stronger with M when $M \le 8$ and stable when $M > 8$; thus, the optimization of *BCE* can be realized more efficiently when $M \le 8$ and becomes less efficient when $M > 8$. Fig. 3 and Table 1 show the

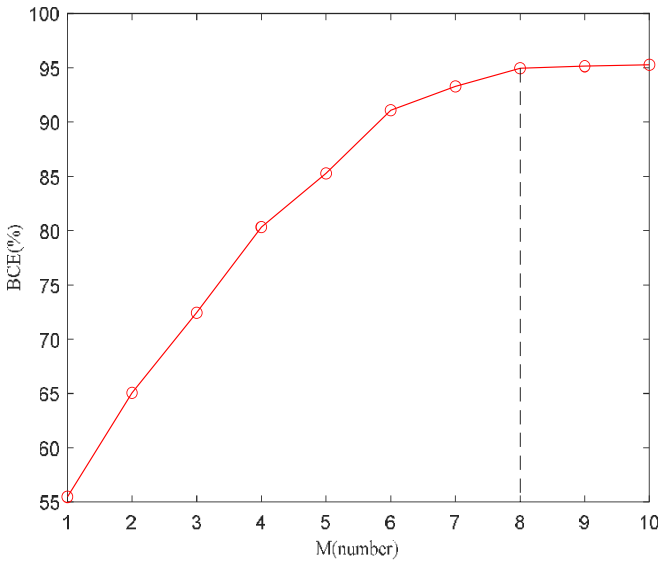

Figure 3. Behaviour of SNANDPA under different number of subarray ($L_x = L_y = 4.5\lambda$, $u_0 = v_0 = 0.2$, $N = 8\times 8$).

Table 1. Synthesis numerical results of SNANDPA under different number of subarray.

$N_x = N_y$	N	M	$u_0 = v_0$	BCE (%)	CSL (dB)
8	64	6	0.2	91.09%	−14.68
8	64	7	0.2	93.28%	−16.03
8	64	8	0.2	94.96%	−17.09
8	64	9	0.2	95.14%	−17.47
For the convenience of the calculation, we set $N_x = N_y$					

behavioral and numerical results of SNANDPA under different numbers of subarray. We conclude that the optimal subarray number $M_{\text{opt}} = 8$ when the element number $N = 8 \times 8$. After repeating the above experiment under different element numbers, the array performance does not improve when M exceeds a certain number. The value of M_{opt} for different element numbers can be determined accordingly.

After determining the optimal subarray number M_{opt} for different element numbers, we further investigate the effect of γ_e on the synthesized results of the SNANDPA model. We select a set of arrays with element numbers of $N \in \{6 \times 6, 7 \times 7, 8 \times 8, 9 \times 9\}$ and subarray number M equal to the corresponding optimal subarray number M_{opt} as determined previously. We find that the performance of the array becomes stronger with N when $N \leq 8 \times 8$ and stable when $N > 8 \times 8$, which means that the optimization of BCE can be realized more efficiently when $N \leq 8 \times 8$ and becomes less efficient when $N > 8 \times 8$. Fig. 4 and Table 2 show the behavioral and numerical results of SNANDPA under different numbers of elements. Finally, we find that the optimal element number N_{opt} is equal to 8×8.

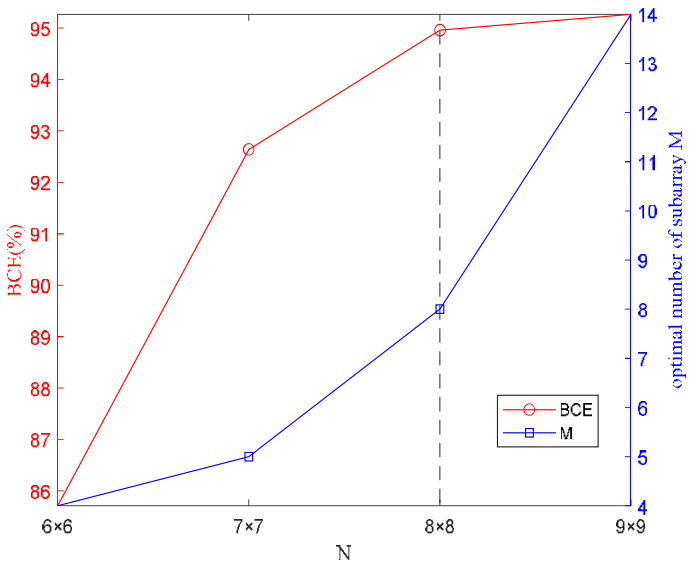

Figure 4. Behaviour of SNANDPA under different numbers of elements and its corresponding value of subarray ($L_x = L_y = 4.5\lambda$, $u_0 = v_0 = 0.2$).

As per the analysis above, we obtain an optimal synthesis model with high array performance (e.g., $[BCE, CSL]|_{N=64}^{\text{SNANDPA}} = [94.96\%, -17.09\,\text{dB}]$) and low cost. Its synthesis layout, excitation model, and power pattern are given in Fig. 5.)

4.2. Comparison of SNANDPA with Other Two Models in Array Performance

After finding the optimal SNANDPA (Subsection 4.1), we compare the proposed model with UANDPA [14] and NAUDPA [19] in terms of array performance. We find that for the same transmitting

Table 2. Synthesis numerical results of SNANDPA under different number of elements.

$N_x = N_y$	N	M_{opt}	$u_0 = v_0$	BCE	CSL
6	36	4	0.2	85.71%	−10.80 dB
7	49	5	0.2	92.64%	−15.57 dB
8	64	8	0.2	94.96%	−17.09 dB
9	81	14	0.2	95.27%	−18.04 dB
For the convenience of the calculation, we set $N_x = N_y$					

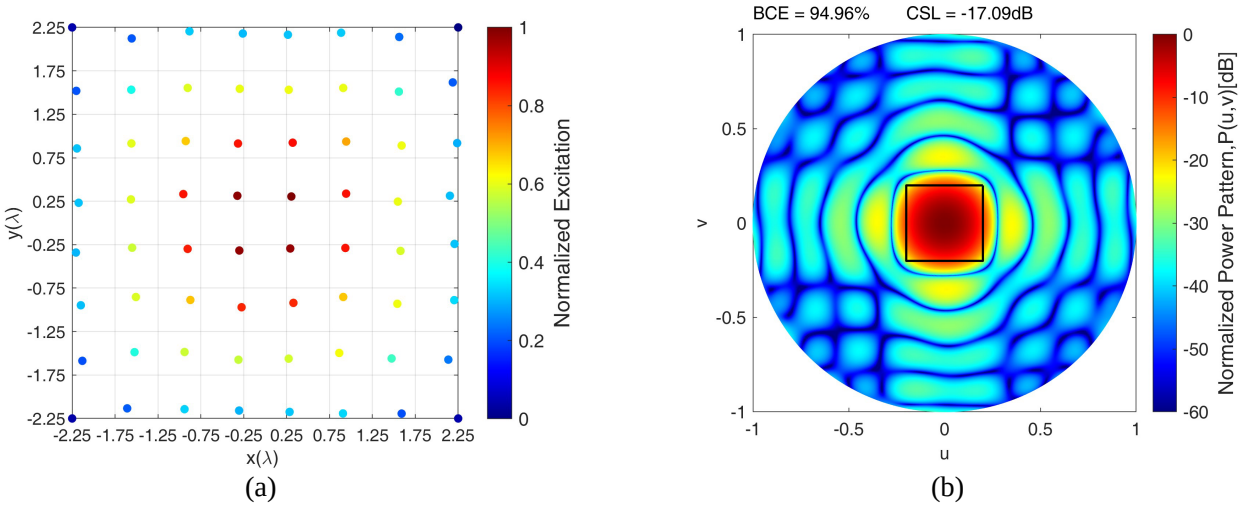

Figure 5. Synthesis result of SNANDPA ($L_x = L_y = 4.5\lambda$, $u_0 = v_0 = 0.2$, $N = 8 \times 8$). (a) Layout and excitation, (b) power pattern.

aperture and receiving region, the nonuniform-amplitude nonuniform-distribution characteristics of the SNANDPA model allow it to efficiently minimize environmental impact while maintaining relatively high energy transmission.

Compared with UANDPA, the proposed model has significantly higher BCE and lower CSL (e.g., $[BCE, CSL]|_{N=64}^{\text{SNANDPA}} = [94.96, -17.09\,\text{dB}]$ vs. $[BCE, CSL]|_{N=100}^{\text{UANDPA}} = [91.06\%, -16.01\,\text{dB}]$, Table 3). Our synthesis results show that BCE of the proposed model is 3.9% higher than that of UANDPA, and CSL of the proposed model is 1.08 dB lower than that of UANDPA. In conclusion, the proposed model can concentrate radiated power more effectively with less environmental impact than UANDPA.

Overall, the proposed model has strong array performance compared with NAUDPA (e.g.,

Table 3. Comparison of synthesis numerical results among SNANDPA, UANDPA and NAUDPA.

	SNANDPA	UANDPA	NAUDPA
N	64	100	100
M	8	1	100
γ_e	64%	100%	100%
γ_a	12.5%	1%	100%
BCE	94.96%	91.06%	96.45%
CSL	−17.09 dB	−16.01 dB	−12.27 dB
$u_0 = v_0 = 0.2, L_x = L_y = 4.5\lambda$			

$[BCE, CSL]|_{N=64}^{\text{SNANDPA}} = [94.96\%, -17.09\,\text{dB}]$ vs. $[BCE, CSL]|_{N=100}^{\text{NAUDPA}} = [96.45\%, -12.27\,\text{dB}]$, Table 3). The synthesis results show that although *BCE* of the proposed model is 1.49% lower than that of UANDPA, and *CSL* of the proposed model is 4.82 dB lower than that of UANDPA; thus, the proposed model has less environmental influence than NAUDPA. In consequence, compared with NAUDPA, the proposed model has a markedly reduced environmental impact while maintaining high *BCE*.

In summary, SNANDPA is more suitable for MPT systems than other two traditional models because it has better array performance.

4.3. Comparison of SNANDPA with Other Two Models in System Cost

For the same transmitting aperture and receiving region, the adoption of sparse array synthesis and subarray partition strategy in SNANDPA reduces the number of array elements and amplifiers.

Unlike UANDPA, due to the sparse characteristics of the proposed model, it can effectively eliminate invalid elements in the transmitting array. The element sparsity γ_e of the proposed model is 36% less than that of UANDPA. The amplifier sparsity γ_a of the proposed model is only 11.5% more than that of UANDPA ($[\gamma_e, \gamma_a]|_{N=64}^{\text{SNANDPA}} = [64\%, 12.5\%]$ vs. $[\gamma_e, \gamma_a]|_{N=100}^{\text{UANDPA}} = [100\%, 1\%]$, Table 3). In conclusion, the proposed model can efficiently reduce the cost of the elements compared to UANDPA while the cost of its amplifiers is relatively low.

Due to the subarray partition technique, compared with NAUDPA, the proposed model has some noticeable differences in terms of excitation. The weight of NAUDPA with the "quasi-Gaussian" excitation is shown in Fig. 6(a), and the weight of SNANDPA with the SAD excitation is shown in Fig. 6(b). We find that element sparsity of the proposed model, γ_e, is 36% less than that of NAUDPA. The amplifier sparsity of the proposed model, γ_a, decreases by 87.5% compared with that of NAUDPA ($[\gamma_e, \gamma_a]|_{N=64}^{\text{SNANDPA}} = [64\%, 12.5\%]$ vs. $[\gamma_e, \gamma_a]|_{N=100}^{\text{NAUDPA}} = [100\%, 100\%]$, Table 3). In summary, the proposed model can efficiently reduce the cost of elements and amplifiers compared to the NAUDPA model.

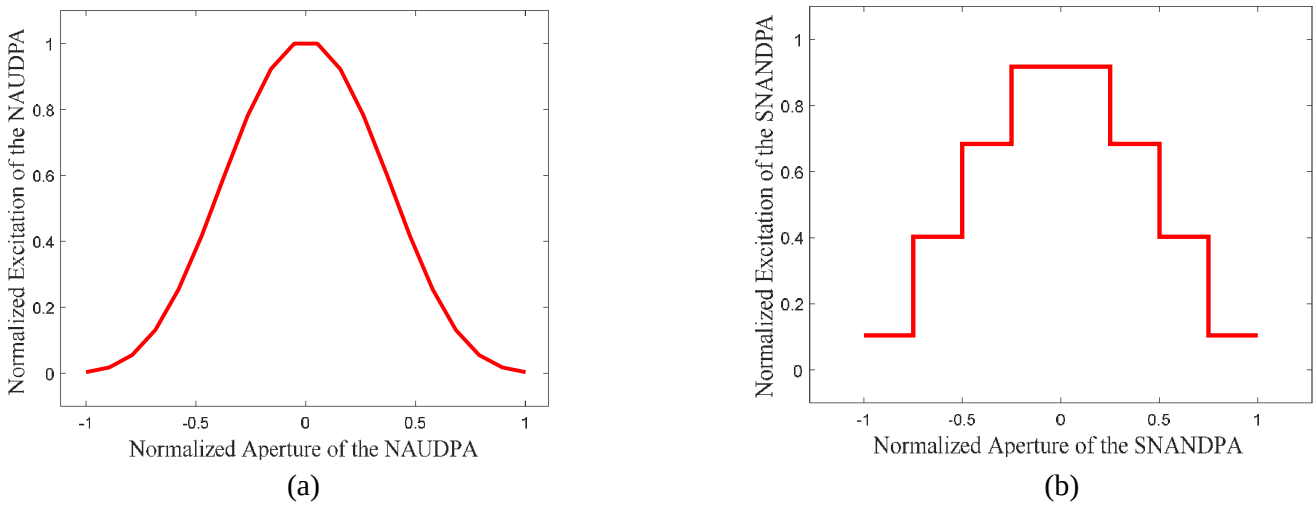

Figure 6. Excitation of NAUDPA and SNANDPA along the axial direction. (a) The weight of NAUDPA ($L_x = L_y = 4.5\lambda$, $u_0 = v_0 = 0.2$, $N = 10 \times 10$) along the axial direction ($x_n = y_n$). (a) The weight of SNANDPA ($L_x = L_y = 4.5\lambda$, $u_0 = v_0 = 0.2$, $N = 8 \times 8$) along the axial direction ($x_n = y_n$).

We conclude that the proposed model has less system cost than other two traditional models. Therefore, SNANDPA can be easily used to establish MPT systems.

4.4. Comparison of DCFPSO with Traditional PSO in Performance

We compare the DCFPSO algorithm applied to SNANDPA synthesis with the other three PSO algorithms to test its stability and efficiency. The results are shown in Fig. 7.

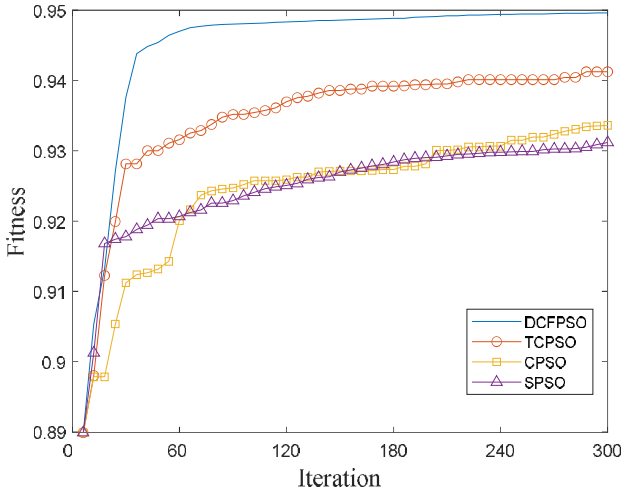

Figure 7. Simulation results of different PSO algorithm ($L_x = L_y = 4.5\lambda$, $u_0 = v_0 = 0.2$, $N = 8 \times 8$).

We find that DCFPSO realizes the optimization of the array synthesis after 230 iterations. The standard particle swarm optimization (SPSO), compressed particle swarm optimization (CPSO), and compressed particle swarm optimization with time-varying acceleration coefficient (TCPSO) have comparatively lower fitness values and slower convergence rates than DCFPSO. The SPSO algorithm targets the relationship between inertia weight and optimization weight and does not consider the relationship between global optimization and local optimization. The CPSO algorithm targets the relationship between global optimization and local optimization, ignoring the influence of inertia weight on the optimization; the algorithm thus converges slowly and falls into the local optima. The TCPSO algorithm includes a time-varying acceleration coefficient based on CPSO, which allows for dynamic adjustment of the inertia weight, global optimization weight, and local optimization weight. Thus, the TCPSO algorithm has better fitness value. The DCFPSO algorithm includes a common compression factor and a time-varying acceleration coefficient, so its global convergence rate is much higher.

5. CONCLUSION

A novel sparse planar array synthesis model with nonuniform-amplitude and nonuniform-distribution, SNANDPA, is developed in this study for MPT applications. We use the DCFPSO algorithm and subarray partition technique to support the proposed model. By means of the DCFPSO algorithm, the proposed method improves array performance by the simultaneous optimization of the distribution and the weight of elements. The feed network is simplified by the subarray partition technique. To this effect, the proposed method simultaneously optimizes array performance and system cost.

We conduct a series of simulations to test the effectiveness of the proposed method. First, we investigate the effects of the ratio of element sparsity γ_e and the ratio of amplifier sparsity γ_a as they both affect the practical application of the proposed method. For example, we can obtain the optimal synthesis model with $\gamma_e = 64\%$ and $\gamma_a = 12.5\%$ when transmitting aperture is $4.5\lambda \times 4.5\lambda$, and receiving region is $u_0 = v_0 = 0.2$. Second, by comparing SNANDPA with the other two planar arrays (UANDPA [14] and NAUDPA [19]), we test the applicability of SNANDPA in MPT systems. We find that SNANDPA has a simpler feed network and similar array performance compared to NAUDPA. SNANDPA has much better array performance and similar system cost compared to UANDPA. Overall, compared with the traditional models, SNANDPA takes into account array performance and the cost of the system in the same time, so it can be better applied in MPT systems.

This is the first time that the DCFPSO algorithm is utilized for array synthesis, so we compare DCFPSO with traditional PSO algorithms in a typical application scenario to evaluate its performance. We find that the DCFPSO algorithm yields a faster convergence rate and higher *BCE* than the other algorithms we tested, suggesting that it is an ideal fit for SNANDPA-based array synthesis in MPT

systems.

In conclusion, the proposed SNANDPA has higher BCE, lower CSL, more concise array arrangement and feed network, and has stronger applicability as a transmitting array of large-scale MPT systems than the other models we tested.

In the future, we will further improve the proposed method from two main perspectives. First, our algorithm does not consider the influence of mutual coupling between array elements on the synthesis results. Although the minimum element spacing limit is set, there is still mutual coupling between array elements. The mutual coupling may distort the actual power pattern of the array, which affects BCE. Therefore, we will consider mutual coupling in our follow-up work. Second, the proposed model is synthesized without error in excitation amplitude and phase. However, in an actual transmitting array, there are random errors in microwave devices that alter the power pattern of the array. We will also consider the influence of random errors generated by excitation amplitude and phase on BCE in our follow-up work.

APPENDIX A. THE CLOSED-FORM SOLUTION OF RECEIVING MATRIX A

According to the definition of receiving matrix **A** and the receiving region as in Eq. (18), we obtain

$$A_{mn} = \int_{-u_0}^{u_0} \int_{-v_0}^{v_0} e^{ik[u(x_m - x_n) + v(y_m - y_n)]} du dv \tag{A1}$$

We can simplify Eq. (A1) as:

$$A_{mn} = \int_{-u_0}^{u_0} e^{iku(x_m - x_n)} du \times \int_{-v_0}^{v_0} e^{ikv(y_m - y_n)} dv \tag{A2}$$

Therefore, the solution of Eq. (A2) in closed form is:

$$A_{mn} = \left(\frac{e^{iku_0(x_m - x_n)} - e^{-iku_0(x_m - x_n)}}{jk(x_m - x_n)} \right) \times \left(\frac{e^{ikv_0(y_m - y_n)} - e^{-ikv_0(y_m - y_n)}}{jk(y_m - y_n)} \right) \tag{A3}$$

For the convenience of calculation, we transform Eq. (A3) into

$$\begin{aligned} A_{mn} &= \left(\frac{2u_0 \sin[ku_0(x_m - x_n)]}{ku_0(x_m - x_n)} \right) \times \left(\frac{2v_0 \sin[kv_0(y_m - y_n)]}{kv_0(y_m - y_n)} \right) \\ &= 4u_0 v_0 \mathrm{sinc}[ku_0(x_m - x_n)] \cdot \mathrm{sinc}[kv_0(y_m - y_n)] \end{aligned} \tag{A4}$$

APPENDIX B. THE CLOSED-FORM SOLUTION OF TRANSMITTING MATRIX B

According to the definition of receiving matrix **B** and the visible range of the array as in Eq. (19), we have

$$B_{mn} = \int_0^{\frac{\pi}{2}} \int_0^{2\pi} e^{ik \sin\theta[(x_m - x_n)\cos\varphi + (y_m - y_n)\sin\varphi]} d\varphi \cdot \sin\theta d\theta \tag{B1}$$

The integrable function can be simplified according to the auxiliary angle formula

$$B_{mn} = \int_0^{\frac{\pi}{2}} \int_0^{2\pi} e^{i\sqrt{[k\sin\theta(x_m - x_n)]^2 + [k\sin\theta(y_m - y_n)]^2} \cdot \sin\left[\varphi + \arctan\left(\frac{k\sin\theta(x_m - x_n)}{k\sin\theta(y_m - y_n)}\right)\right]} d\varphi \cdot \sin\theta d\theta \tag{B2}$$

According to the periodicity of definite integral, we can convert the upper and lower limit $\{\varphi : \varphi \in [0, 2\pi]\}$ of internal integral into $\{\varphi : \varphi \in [-\pi, \pi]\}$

$$B_{mn} = \int_0^{\frac{\pi}{2}} \int_{-\pi}^{\pi} e^{i\sqrt{[k\sin\theta(x_m - x_n)]^2 + [k\sin\theta(y_m - y_n)]^2} \cdot \sin\left[\varphi + \arctan\left(\frac{k\sin\theta(x_m - x_n)}{k\sin\theta(y_m - y_n)}\right)\right]} d\varphi \cdot \sin\theta d\theta \tag{B3}$$

Since the 0-th order Bessel function of argument β is defined as

$$J_0(\beta) \frac{1}{2\pi} \int_{-\pi}^{\pi} e^{i\beta\sin\varphi} d\varphi, \tag{B4}$$

we can simplify Eq. (B3) as

$$\begin{aligned} B_{mn} &= 2\pi \int_0^{\frac{\pi}{2}} J_0 \left\{ \sqrt{[k\sin\theta(x_m - x_n)]^2 + [k\sin\theta(y_m - y_n)]^2} \right\} \sin\theta d\theta \\ &= 2\pi \int_0^{\frac{\pi}{2}} J_0[k\sin\theta\sqrt{(x_m - x_n)^2 + (y_m - y_n)^2}] \sin\theta d\theta \end{aligned} \tag{B5}$$

By Taylor expansion of the 0-th order Bessel function, we can further simplify Eq. (B5) as

$$\begin{aligned} B_{mn} &= 2\pi \cdot \sum_{m=0}^{\infty} \frac{(-1)^m \left(k\sqrt{(x_m - x_n)^2 + (y_m - y_n)^2}\right)^{2m}}{(m!)^2 2^{2m}} \cdot \int_0^{\frac{\pi}{2}} \sin^{2m+1}\theta d\theta \\ &= 2\pi \cdot \sum_{m=0}^{\infty} \frac{(-1)^m \left(k\sqrt{(x_m - x_n)^2 + (y_m - y_n)^2}\right)^{2m}}{(m!)^2 2^{2m}} \cdot \frac{(2m)!!}{(2m+1)!!} \\ &= \pi \cdot \sum_{m=0}^{\infty} (-1)^m \frac{(k\sqrt{(x_m - x_n)^2 + (y_m - y_n)^2})^{2m}}{(2m+1)!} \cdot \underbrace{\frac{(2m+1)!(2m)!!}{(2m+1)!!(m!)^2 2^{2m-1}}}_{=2} \\ &= 2\pi \cdot \sum_{m=0}^{\infty} (-1)^m \frac{(k\sqrt{(x_m - x_n)^2 + (y_m - y_n)^2})^{2m}}{(2m+1)!} \end{aligned} \tag{B6}$$

Notice that the sinc function is defined as

$$\mathrm{sinc}(x) \triangleq \frac{\sin x}{x} = \sum_{m=0}^{\infty} (-1)^m \frac{x^{2n}}{(2n+1)!} \tag{B7}$$

Therefore, we can simplify Eq. (B6) as

$$\begin{aligned} B_{mn} &= 2\pi \cdot \sum_{m=0}^{\infty} (-1)^m \frac{(k\sqrt{(x_m - x_n)^2 + (y_m - y_n)^2})^{2m}}{(2m+1)!} \\ &= 2\pi \cdot \frac{\sin(k\sqrt{(x_m - x_n)^2 + (y_m - y_n)^2})}{k\sqrt{(x_m - x_n)^2 + (y_m - y_n)^2}} \\ &= 2\pi \cdot \mathrm{sinc}(k\sqrt{(x_m - x_n)^2 + (y_m - y_n)^2}) \end{aligned} \tag{B8}$$

ACKNOWLEDGMENT

This work was supported by the National Natural Science Foundation of China (Grant No. 51877151) and the Program for Innovative Research Team in University of Tianjin (Grant No. TD13-5040).

REFERENCES

1. Cheng, C., F. Lu, Z. Zhou, et al., "Load-independent wireless power transfer system for multiple loads over a long distance," *IEEE Transactions on Power Electronics*, Vol. 34, No. 9, 9279–9288, 2019.
2. Nakamoto, Y., N. Hasegawa, Y. Takagi, et al., "A study on microwave power transfer to rectangular antenna for stratospheric platform," *2019 IEEE Asia-Pacific Microwave Conference (APMC)*, 996–998, 2019.
3. Lee, C. H., G. Jung, K. A. Hosani, et al., "Wireless power transfer system for an autonomous electric vehicle," *2020 IEEE Wireless Power Transfer Conference*, 467–470, 2020.
4. Lu, F., H. Zhang, W. Li, et al., "A high-efficiency and long-distance power-relay system with equal power distribution," *IEEE Journal of Emerging and Selected Topics in Power Electronics*, Vol. 8, No. 2, 1419–1427, 2020.

5. Nakamoto, Y., N. Hasegawa, Y. Ohta, and N. Shinohara, "A study on microwave power transmission system to high altitude platform station considering rectification efficiency," *2020 IEEE Asia-Pacific Microwave Conference*, 187–189, 2020.
6. Massa, A., G. Oliveri, F. Viani, and P. Rocca, "Array designs for long-distance wireless power transmission: State-of-the-art and innovative solutions," *Proceedings of the IEEE*, Vol. 101, No. 6, 1464–1481, 2013.
7. Rocca, P., G. Oliveri, and A. Massa, "Array synthesis for optimal wireless power systems," *2014 IEEE Antennas and Propagation Society International Symposium*, 1407–1408, 2014.
8. Shinohara, N., "History of research and development of beam wireless power transfer," *2018 IEEE Wireless Power Transfer Conference*, 1–4, 2018.
9. Shinohara, N., "Wireless power transfer in Japan: Regulations and activities," *2020 14th European Conference on Antennas and Propagation (EuCAP)*, 1–4, 2020.
10. Shinohara, N., "History and innovation of wireless power transfer via microwaves," *IEEE Journal of Microwaves*, Vol. 1, No. 1, 218–228, 2021.
11. Li, X., B. Duan, J. Zhou, et al., "Planar array synthesis for optimal microwave power transmission with multiple constraints," *IEEE Antennas and Wireless Propagation Letters*, Vol. 16, 70–73, 2017.
12. Zhou, H., X. Yang, and S. Rahim, "Array synthesis for optimal microwave power transmission in the presence of excitation errors," *IEEE Access*, Vol. 6, 27433–27441, 2018.
13. Li, X., K. M. Luk, and B. Duan, "Multiobjective optimal antenna synthesis for microwave wireless power transmission," *IEEE Transactions on Antennas and Propagation*, Vol. 67, No. 4, 2739–2744, 2019.
14. Chatterjee, S., S. Chatterjee, B. Bandyopadhyay, and A. Majumder, "Simultaneous control of side lobe level and beamwidth in planar array antenna using restricted search evolutionary algorithms," *2019 IEEE Asia-Pacific Microwave Conference*, 673–675, 2019.
15. Lopez, P., J. A. Rodriguez, F. Ares, and E. Moreno, "Subarray weighting for the difference patterns of monopulse antennas: Joint optimization of subarray configurations and weights," *IEEE Transactions on Antennas and Propagation*, Vol. 49, No. 11, 1606–1608, 2001.
16. Li, X., B. Duan, and L. Song, "Design of clustered planar arrays for microwave wireless power transmission," *IEEE Transactions on Antennas and Propagation*, Vol. 67, No. 1, 606–611, 2019.
17. Cui, C., Y. Jiao, L. Zhang, et al., "Synthesis of subarrayed monopluse arrays with contiguous elements using a DE algorithm," *IEEE Transactions on Antennas and Propagation*, Vol. 65, No. 8, 4340–4345, 2017.
18. Prasad, S., "On the index for array optimization and the discrete prolate spheroidal functions," *IEEE Transactions on Antennas and Propagation*, Vol. 30, No. 5, 1021–1023, 1982.
19. Oliveri, G., L. Poli, and A. Massa, "Maximum efficiency beam synthesis of radiating planar arrays for wireless power transmission," *IEEE Transactions on Antennas and Propagation*, Vol. 61, No. 5, 2490–2499, 2013.
20. Ratnaweera, A., S. K. Halgamuge, and H. C. Watson, "Self-organizing hierarchical particle swarm optimizer with time-varying acceleration coefficients," *IEEE Transactions on Evolutionary Computation*, Vol. 8, No. 3, 240–255, 2004.
21. Banerjee, C. and R. Sawal, "PSO with dynamic acceleration coefficient based on mutiple constraint satisfaction: Implementing fuzzy inference system," *2014 International Conference on Advances in Electronics Computers and Communications*, 1–5, 2014.
22. Yang, J., S. Yang, and P. Ni, "A vector tabu search algorithm with enhanced searching ability for pareto solutions and its application to multiobjective optimizations," *IEEE Transactions on Magnetics*, Vol. 52, No. 3, 1–4, 2016.
23. Rocca, P., G. Oliveri, and A. Massa, "Innovative array designs for wireless power transmission," *International Microwave Workshop Series on Innovative Wireless Power Transmission: Technologies, Systems, and Applications*, 2011.

24. Morabito, A. F., A. R. Laganà, and T. Isernia, "Optimizing power transmission in given target areas in the presence of protection requirements," *IEEE Antennas and Wireless Propagation Letters*, Vol. 14, 44–47, 2014.
25. Li, J., J. Pan, and X. Li, "A novel synthesis method of sparse nonuniform-amplitude concentric ring arrays for microwave power transmission," *Progress In Electromagnetics Research C*, Vol. 107, 1–15, 2021.
26. Zhou, H. W., X. X. Yang, and S. Rahim, "Synthesis of the sparse uniform-amplitude concentric ring transmitting array for optimal microwave power transmission," *International Journal of Antennas & Propagation*, 2018.
27. Qiao, X.-L. and Chen, "Sparse antenna array design for MIMO radar using multiobjective differential evolution," *International Journal of Antennas & Propagation*, 2016.